NRC·CNRC

NRC Publications Archive
Archives des publications du CNRC

Mechanistic insight into Bis(amino) copper formate thermochemistry for conductive molecular ink design

Shin, Homin; Liu, Xiangyang; Lacelle, Thomas; Macdonell, Ryan J.; Schuurman, Michael S.; Malenfant, Patrick R. L.; Paquet, Chantal

This publication could be one of several versions: author's original, accepted manuscript or the publisher's version. / La version de cette publication peut être l'une des suivantes : la version prépublication de l'auteur, la version acceptée du manuscrit ou la version de l'éditeur.
For the publisher's version, please access the DOI link below./ Pour consulter la version de l'éditeur, utilisez le lien DOI ci-dessous.

Publisher's version / Version de l'éditeur:
https://doi.org/10.1021/acsami.0c08645
ACS Applied Materials & Interfaces, 12, 29, pp. 33039-33049, 2020-06-26

NRC Publications Archive Record / Notice des Archives des publications du CNRC :
https://nrc-publications.canada.ca/eng/view/object/?id=350191c2-d8e1-4173-b1bc-d7c4dadbbd81
https://publications-cnrc.canada.ca/fra/voir/objet/?id=350191c2-d8e1-4173-b1bc-d7c4dadbbd81

Access and use of this website and the material on it are subject to the Terms and Conditions set forth at
https://nrc-publications.canada.ca/eng/copyright
READ THESE TERMS AND CONDITIONS CAREFULLY BEFORE USING THIS WEBSITE.

L'accès à ce site Web et l'utilisation de son contenu sont assujettis aux conditions présentées dans le site
https://publications-cnrc.canada.ca/fra/droits
LISEZ CES CONDITIONS ATTENTIVEMENT AVANT D'UTILISER CE SITE WEB.

Questions? Contact the NRC Publications Archive team at PublicationsArchive-ArchivesPublications@nrc-cnrc.gc.ca. If you wish to email the authors directly, please see the first page of the publication for their contact information.

Vous avez des questions? Nous pouvons vous aider. Pour communiquer directement avec un auteur, consultez la première page de la revue dans laquelle son article a été publié afin de trouver ses coordonnées. Si vous n'arrivez pas à les repérer, communiquez avec nous à PublicationsArchive-ArchivesPublications@nrc-cnrc.gc.ca.

National Research Council Canada | Conseil national de recherches Canada

Canada

Mechanistic Insight into Bis(amino) Copper Formate Thermochemistry for Conductive Molecular Ink Design

Homin Shin,[1]* Xiangyang Liu,[1] Thomas Lacelle,[1] Ryan J. MacDonell,[2] Michael S. Schuurman,[1,2] Patrick R. L. Malenfant,[1] Chantal Paquet[1]**

[1] National Research Council of Canada, 100 Sussex Drive, Ottawa, ON, K1A 0R6, Canada

[2] Department of Chemistry and Biomolecular Sciences, University of Ottawa, Ottawa, ON, K1N 6N5, Canada

ABSTRACT

Increasing attention has been given to amine-copper formate complexes for their use as low cost printable conductive inks. The structure of amine ligands coordinated to copper centers has been reported to dictate the properties of copper molecular inks, such as stability and printability, thereby influencing the copper reduction pathway during the thermolysis. Yet, the underlying mechanism by which formate is oxidized when complexed with amine ligands is still not fully understood. Here, we propose a mechanistic pathway of copper formate dehydrogenation and decarboxylation and the critical role that amine ligands play in their thermal decomposition by employing first-principles electronic structure computations and experimental analysis of thermolysis reactions. Based on the computational characterization of the relevant reaction pathways for a number of primary, and secondary amine, as well as pyridine ligand complexes, we are the first to show that the hydrogen bonds formed between the amine ligand and formate are the key factors governing the activation energy, providing a design principle for the synthesis of organic ligands that can tune the height of the reaction barriers of the dehydrogenation and decarboxylation reactions. The calculations, confirmed by NMR studies, show that the reduction of Cu(II) to Cu(I) occurs in concert with the release of H_2 via the dimerization of Cu(II) hydride. This result suggests that the monomeric elimination of H_2 is not favorable for the Cu(II) to Cu(I) reduction, and thus identifies *dimeric* amino copper formate as an important intermediate for copper reduction, whose thermodynamic stabilities are also dictated by the nature of the amine ligands.

KEYWORDS

Printed electronics, Conductive inks, Copper formate, Amine ligands, Rate-determining step

INTRODUCTION

Amine-coordinated copper formate compounds are the basis of many printable molecular inks used to fabricate low cost electronic devices.[1–15] These copper molecular inks convert to copper metal upon heating to yield films with high electrical conductivities. Many of the advantages of these inks are derived from their molecular nature, and thus molecular tailoring of the amine ligand may be used to improve the stability and printability of the ink. For instance, the basicity, degree of steric hindrance, molecular weight, and stoichiometry of amine ligands bound to copper formate have been shown to govern the copper particle sizes, film morphologies and porosity that ultimately determine the electrical properties of the copper films.[16–24]

The nature of the amine ligand complexed to copper formate has also been shown to dictate the temperature at which these compounds decompose into copper films, an important feature for tuning the processing temperatures of printed circuits on plastic substrates.[1-5,7-9,12] It was proposed that hexylamine donates electrons to copper ions resulting in the partial reduction of the Cu(II) center, which facilitates the release of the neutral HCOO, thus lowering the reduction temperature of the Cu(II) formate.[5] Recently, we have shown that the pyridine derivatives have lower decomposition temperatures than the alkylamine analogues,[7] and subsequently reported that bis(amino) copper formates decompose in a temperature range that depends on the possible number of hydrogen bonds that can be formed between the amine and formate ligands.[8] Marchal *et. al.*[12] have suggested that the amine ligands coordinated to the copper formate center determines the structural similarities between the Cu(II) and Cu(I) compounds and the relative stabilities of Cu(I) intermediates, both of which affect the temperature at which the compounds reduce to metallic copper. Although these reports highlight the central role of the amine ligands in the thermolysis of copper-formate compounds, a first-principles computation-based, full understanding of the mechanistic pathway by which the amine-bound copper formate compounds reduce to copper films has remained elusive.

In the absence of amine ligands, it has been known that anhydrous Cu(II) formates thermally decompose into Cu(0), CO_2 and H_2 via the two distinct, but partially overlapping stepwise reductions of Cu(II)→Cu(I)→Cu(0), in which the intermediate Cu(I) exhibits a slightly lower relative reactivity than its Cu(II) counterpart.[25-26] Molecular ink decomposition also involves the decarboxylation and dehydrogenation of formate to form CO_2 and H_2, yet in the presence of functional amine ligands directly coordinated to the copper center. Therefore, it is

expected that the nature of the amines influences the course of reduction pathways by either delaying or facilitating a certain reduction reaction step via possible intermediate formation. Studies aimed at elucidating the catalytic conversion from metal formate complexes to H_2 and CO_2 and vice versa, have provided insight into how ligands influence the mechanism of formate decarboxylation and dehydrogenation on these metal centers.[27] Ravasio *et al.* demonstrated that the reactivity of formic acid dehydrogenation by Cu-amino based systems varies depending on the basicity of the amine with more basic amines favoring higher conversion activity.[28] In a follow-up computational study, it was shown that amine dissociation followed by β-hydride transfer is the key intermediate step in copper catalyzed decomposition of formate, thereby governing the catalyst's activity, in which amine basicity, steric properties as well as amine binding ability, influence the dehydrogenation reaction.[29] These reports illustrate that the ligands on the copper center direct the decarboxylation and dehydrogenation of formate to form CO_2 and H_2, yet there is currently an incomplete understanding of the mechanistic details by which these processes occur – details that would inform the design of amine ligand structures in order to synthesize copper formate complexes with advantageous thermal (decomposition temperature) properties. In particular, identifying the key reaction intermediates, their structures and relative stabilities would elucidate the role of amines in facilitating the liberation of CO_2 and H_2, and how they govern the sequence of thermolysis reactions, which would greatly affect the quality of the resulting copper films as a result.

In this study, we employ a variety of quantum chemical methods, in conjunction with experimental diagnostics that include differential scanning calorimetry (DSC), thermogravimetric analysis coupled to Fourier transform infrared absorption spectroscopy and mass spectrometry (TGA-FTIR-MS), as well as nuclear magnetic resonance (NMR) studies, in order to elucidate the mechanistic details of the thermal decomposition of bis(amino) copper formate complexes on their way to forming Cu(I), CO_2 and H_2. The elucidation of the reaction pathway provided here, which reveals how amines guide the formation of the transition states and direct the formation and stability of reaction intermediates, will shed light on the purposeful design of ligands to minimize the reaction barriers and to control the stability of intermediates, thereby providing the design principles critical to synthesize copper-based molecular inks with optimized thermal profiles for metallization.

RESULTS AND DISCUSSION

Recently, we reported that the decomposition temperature of bis(amino) copper formates is controlled by the structure of the amine ligands.[8] As highlighted in Figure 1, the TGA-FTIR analysis and optical images of copper-formate compounds at incremental temperatures shows that the nature of amine ligands – primary amines, secondary amines, and pyridines – coordinated to the copper center strongly influences at what temperature CO_2 is released, thereby impacting their reduction temperature of Cu(II) to Cu(I). While the differences in the decomposition temperatures among those three classes of complexes were observed to be notable, crystal structures resolved by single-crystal X-ray diffraction[7-8] showed that they all possess a similar coordination geometry: the central copper atom is directly coordinated with two nitrogen atoms from two monodentate amine ligands and two oxygen atoms from two respective formates, whereas the two other formate oxygens are weakly bonded to the copper. Thus, as also supported by our FTIR data (see Figure S1), the complexes studied in this work do not form a coordination network, but rather exist as discrete molecules. This coordination geometry is in a contrast with anhydrous Cu(II) formates consisting of three-dimensional polymeric networks, in which the copper ions are bridged by the formate ions – each copper ion is linked to four other coppers by four different formate groups.[30] We note that it could be one way to rationalize why anhydrous copper (II) formate has a higher decomposition temperature compared to amine complexes, as additional thermal energy will be needed to break the infinitely bridged copper-formates networks into monomeric complexes. However, the mechanistic details which lead to the different thermal decomposition temperature among bis(amino) copper formates whose initial compounds possess a similar coordinate geometry still need to be elucidated.

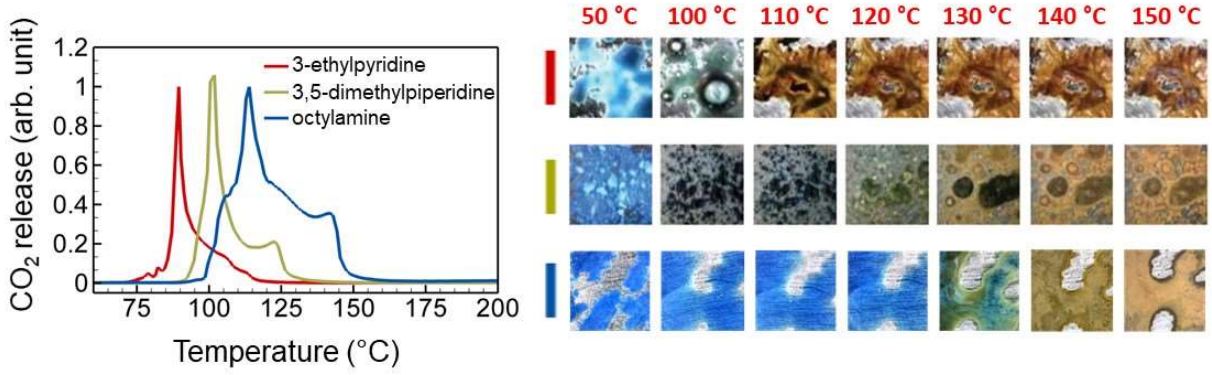

Figure 1. Comparison of the CO_2 release during thermolysis of copper formate coordinated to primary amine ligands (octylamine, blue curve), secondary amine ligands (3,5-dimethylpiperidine, yellow curve)

and pyridine ligands (3-ethylpyridine, red curve). The optical images of the three compounds at incremental temperatures are also presented.

The rate-determining intramolecular rearrangement

Our computations consider three different classes of amine ligands coordinated to the copper formate: methylamine as a primary amine (PA), dimethylamine as a secondary amine (SA), and pyridine as a heterocyclic amine (PYR).[31] The nuclear structures of these compounds are optimized using density functional theory (DFT) and are shown in the first column of Figure 2. Their coordination structures are in agreement with crystal structures resolved by single-crystal X-ray diffraction.[7-8] The reaction of formate by direct dissociation into a neutral radical HCOO was found to be energetically unfavorable. Alternatively, the lowest barrier to reaction is predicted to be CO_2 elimination, following intramolecular rearrangement. To investigate the role of amine ligands in this process, particularly in the rotation of formate as a potential rate-determining step, minimum energy paths were optimized between the ground-state configuration of the compound (i.e., reactant) and the optimized H-bound formate intermediate (i.e., product) employing the climbing image nudged elastic band (NEB) method. The relative orientation of formate in the reactants, products, and the two representative converged intermediates along the minimal energy paths for three types of Cu-amine complexes are illustrated in Figure 2 and showcase the different reaction pathways guided by the different amine ligands.

The results of these computations suggest that there exist (at least) two distinct internal rotation pathways which are characterized by the number of hydrogen bonds that can form between the amine ligand and formate. As displayed in Figure 2, one pathway (denoted by R_I) involves rotation about an axis so as to maintain the hydrogen bond formed between the amine H and the formate O atom, while the other (denoted by R_{II}) involves a free rotation of the formate in the absence of an H-bonding interaction. The Cu-PA complex, which has the possibility of forming two hydrogen bonds, follows the R_I pathway; the molecular plane of the formate flips 180º with respect to one of the C-O bonds in the formate, while maintaining the hydrogen bond throughout the rotation. This rotation is accompanied by breaking the Cu-O coordination bond, which is mediated by another weakly formed hydrogen bond (red dotted line in Figure 2) with the second methylamine at the transition state. Conversely, the Cu-PYR complex with no formate-ligand hydrogen bonds undergoes the R_{II} pathway; a formate freely rotates to minimize the Cu-O coordination distance, allowing the formate H to approach the Cu center. It was observed that the

Cu-SA complex can undergo both rotational pathways, either by utilizing the one possible hydrogen bond, similar to that of Cu-PA, or by breaking the hydrogen bond and taking the free rotation path, similar to that of Cu-PYR. Note that Cu-PA is unlikely to follow the R_{II} pathway as it is highly hindered due to another available hydrogen bond that can be formed with the opposite ligand upon such rotation.

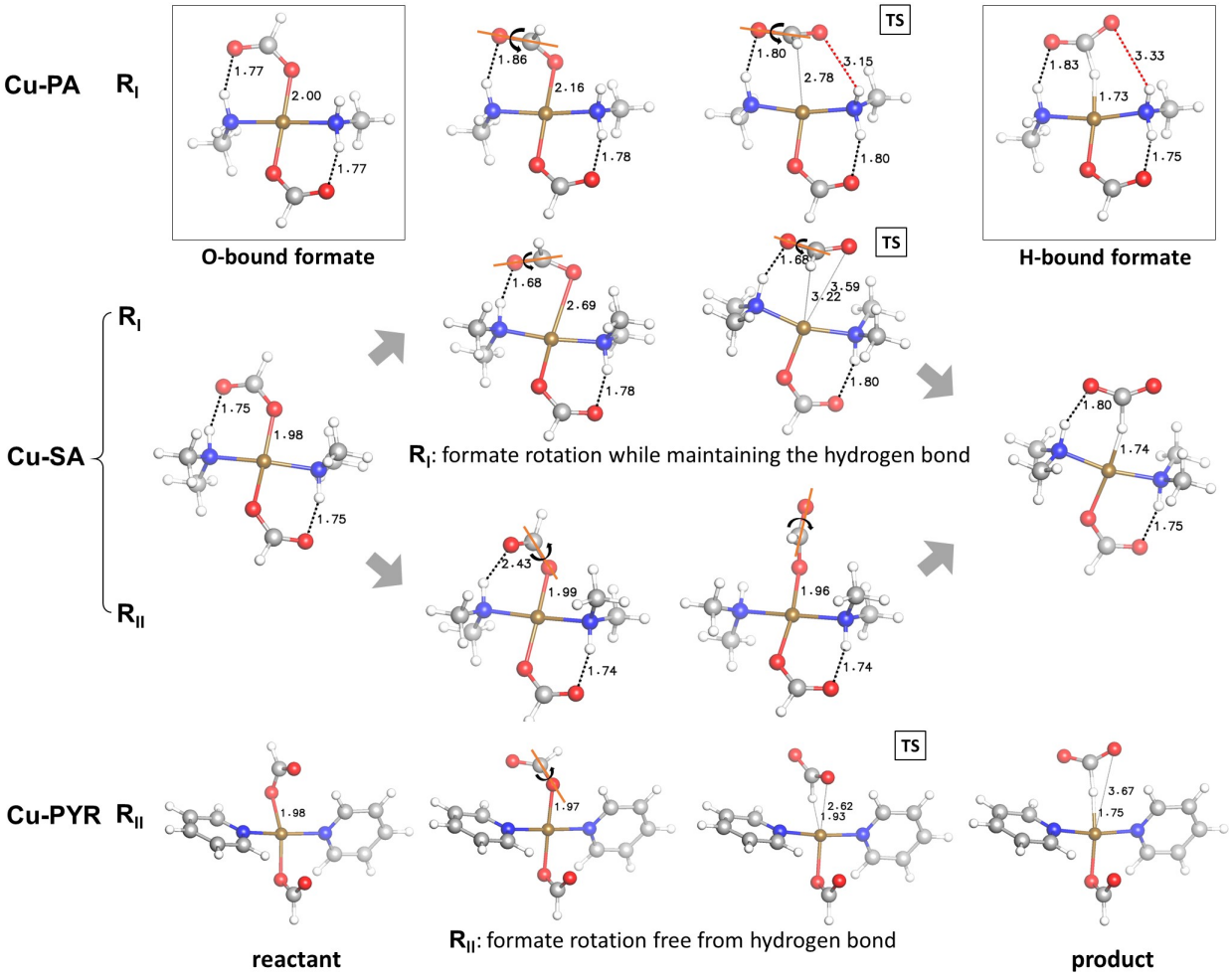

Figure 2. Minimum energy pathways of rotating the O-bound formate to the H-bound formate in the complexes of Cu-PA, Cu-SA, and Cu-PYR. The two different rotational pathways are denoted by R_I and R_{II}. The converged highest saddle points of transition states (TS) are also displayed.

The energy barriers of the transition states (TS) for the three representative Cu-amine complexes were obtained from the calculated minimum energy path of reactions using 4 intermediate images. As shown in Figure 3, the results reveal that the height of the activation

energy barrier is determined by the formate rotational motion. First, the energy barrier was found to be higher for Cu-PA complex than Cu-PYR, as the hydrogen bonds hinder the free rotation of formate. This implies that a higher temperature is required to activate the decarboxylation of formate on compounds with ligands analogous to PA (*i.e.* primary amines) than ligands analogous to pyridines. The barrier height of the Cu-SA following the R_I pathway is slightly lower than that of the Cu-PA, whilst the reaction of Cu-SA following the R_{II} pathway is shown to be almost barrierless. From the vibrational frequency calculations, all transition state structures of the Cu-PA, Cu-PYA, and Cu-SA with the R_I pathway were verified by the existence of only one imaginary frequency; however, the R_{II} reaction pathway of Cu-SA was shown not to possess a true transition state (no imaginary frequency has been observed). This indicates that for the R_{II} pathway of Cu-SA, the formate rotation is not the rate-determining step. As will be discussed shortly, the H-bound formate product releases CO_2 as the next step of the reaction, a reaction step that is endothermic for all three complexes (see Table 1). For the R_{II} pathway of Cu-SA, the release of CO_2 ($\Delta E_{SA}^{CO2} = 23.4$) is the highest energy level, thus resulting in the rate-determining step. By considering all the barrier heights of the rate-determining step, the order of activation energy barrier heights in decreasing order is: Cu-PA ($\Delta E_{PA}^{\ddagger} = 27.1$) > Cu-SA ($\Delta E_{SA1}^{\ddagger} = 26.5$ for R_I) > Cu-PYR ($\Delta E_{PYR}^{\ddagger} = 22.2$). For Cu-SA, the possible reaction route is likely the mixture of the two different pathways of R_I and R_{II}, in which both of their highest energy barriers to overcome are lower than the Cu-PA and higher than the Cu-PYR. A previous study on formate dehydrogenation (using Pd catalysts) suggested the rotational barrier of formate interacting with primary amines is lower than that with secondary or tertiary amines, due to the steric hindrance that they experience from the amine ligands.[32] However, the present case of bis(amino) copper formates demonstrates that the energy cost of formate rotation is not solely determined by the steric hindrance, but more dominantly by the presence of hydrogen bonds, in which the hydrogen bonding interaction is the primary determining factor of the rate-determining barrier heights.

Our results show that it is the rearrangement of the formate ligands that is the rate-determining step along the reaction pathway. The order of decomposition temperature shown in Figure 1 (Cu-octylamine>Cu-3,5-dimethylamine>Cu-3-ethylpyridine) is in good agreement with the theory calculations of activation energy, which estimated that the order of barrier heights is Cu-PA>Cu-SA>Cu-PYR. With respect to ligand selection for copper formate-based molecular inks, it will likely prove desirable to minimize the possibility of intramolecular hydrogen bonding

between the ligand and the formate, and thus ensure that the processing temperatures required to reduce the copper complexes are also lowered.

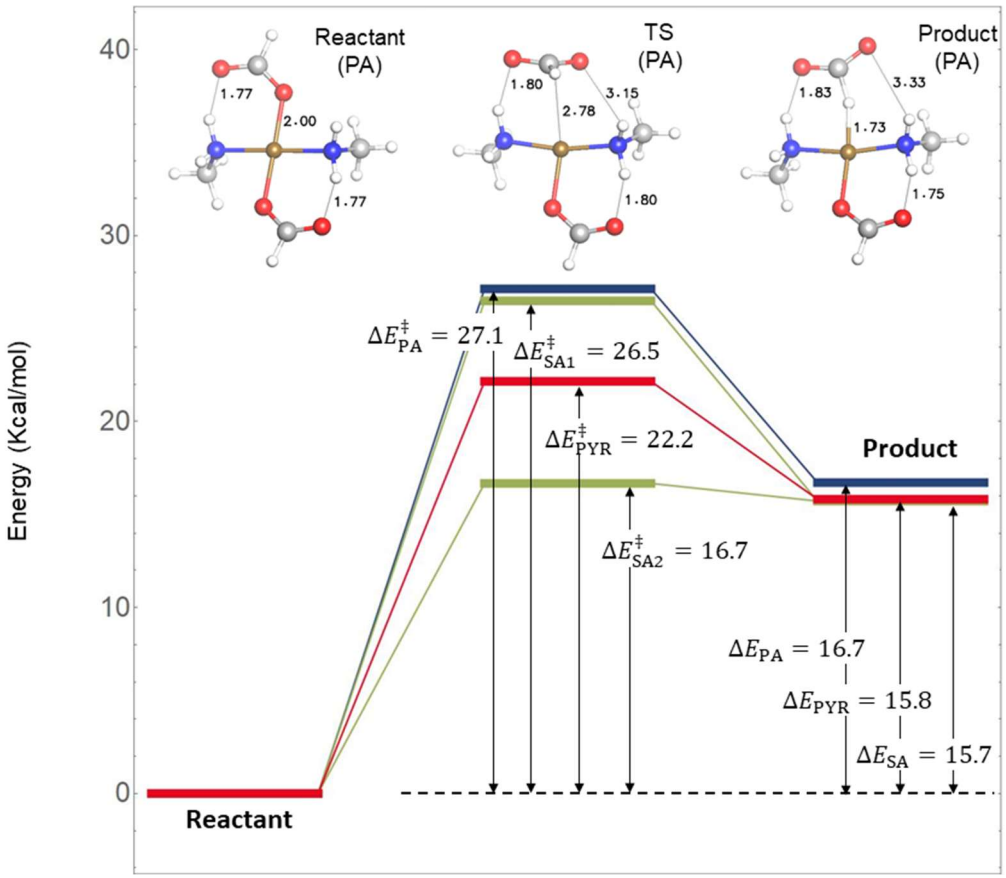

Figure 3. The activation energy barriers of the formate rotation in the copper complexes with primary methylamine (PA), secondary dimethylamine (SA) and pyridine (PYR) are plotted in blue, green and red, respectively.

Our results are consistent with previous work on the metal-catalyzed CO_2 reduction or H_2 production via formate-metal mediated catalysis. It has been reported previously that rearrangement from the O-bound to the H-bound formate complex is the key reaction step to facilitate decarboxylation and dehydrogenation of formic acid, while the conversion from the H-bound to the O-bound formate species is required for the hydrogenation of CO_2 to formic acid.[33-39] Schmeier *et al*.[34] proposed that such transformations occur via metal-formate dissociation of the H-bound formate complex to form a formate ion, followed by subsequent re-coordination as an O-bound species; however, the mechanism by which the complex successfully re-coordinates with the desired orientation is not clear. While it has been previously shown that formate ligands

may rotate in such a way that the hydrogen approaches toward the vacant site at the metal center, thereby allowing β-hydride elimination, this rotation pathway is energetically unfavorable when the complexes have their coordination sphere highly saturated, or when the formate has formed intramolecular hydrogen bonds with other ligands, as is the case with the bis(amino) copper complex studied herein. Since the motion of the formate ligand is restricted by hydrogen bonding interactions, the minimum energy pathway for the formate is an "out-of-plane" rotation as shown in Figure 2, which is distinct from the "in-plane" rotation as commonly shown for β-hydride elimination. A schematic is provided in Figure S4 to clearly describe the difference between "out-of-plane" and "in-plane" rotations that transform the O-bound to H-bound formate configuration. We have shown that for such compounds, the transformation between the H-bound and O-bound formate is largely controlled by the hydrogen bonding capacity of the ligands, which in turn determines the activation energy of the rate determining step involving the decarboxylation reaction and formation of the metal hydride. Our results thus suggest that the conversion efficiency (from formate to H_2 and CO_2 and vice versa) of copper formate compounds would be also tuned via intramolecular bonding interactions between formate and ligands, as well as by the strength of the hydrogen-bonding interactions that ultimately dictate the activation barrier of the rate-determining formate rotation.

Mechanisms for thermal decomposition

Following formation of the H-bound formate product, which we predict to be the highest-energy barrier, subsequent mechanistic steps involve the release of H_2, removal of the amine ligands, and ultimate reduction of the Cu center via thermal decomposition. The current computations suggest a reaction sequence, depicted in Figure 4, in which CO_2 dissociation (ΔE_{CO_2}) is followed by dimerization (ΔE_{dim}) which gives rise to H_2 release (ΔE_{H_2}) and finally ligand dissociation (ΔE_{2L}) upon heating of the copper-formate-PA complex (see Scheme 1).

The first endothermic reaction is attributed to the CO_2 release from the starting precursor compound yielding a Cu(II)-hydride. Assuming that ligand dissociation follows promptly from this step, our computations show that this process would involve a large enthalpic cost $\Delta E_L = 16.8$kcal/mol. Alternatively, the dimerization reaction forming the Cu(II)-Cu(II) bonded dimeric complex was found to be exothermic with a large energy gain of $\Delta E_{dim} = -26.7$ kcal/mol, suggesting that dimerization is spontaneous. The dimeric compounds subsequently produce H_2,

which reduces the dimeric Cu(II)-Cu(II) complex forming a dimeric Cu(I)-Cu(I) compound with high thermodynamic stability (see Figure S5 for optimized structures of dimer compounds). It is expected that the mononuclear pathway for the elimination of H_2 is not favorable, as it needs to undergo a second decarboxylation from the monomeric Cu(II)-hydride, which requires it to overcome almost the same size of energy barrier associated with the formate rearrangement. The fact that reduction of Cu(II) to Cu(I) occurred at the dimeric stage also implies that the nucleation of Cu particles could start to grow before the complete reduction to Cu(0).

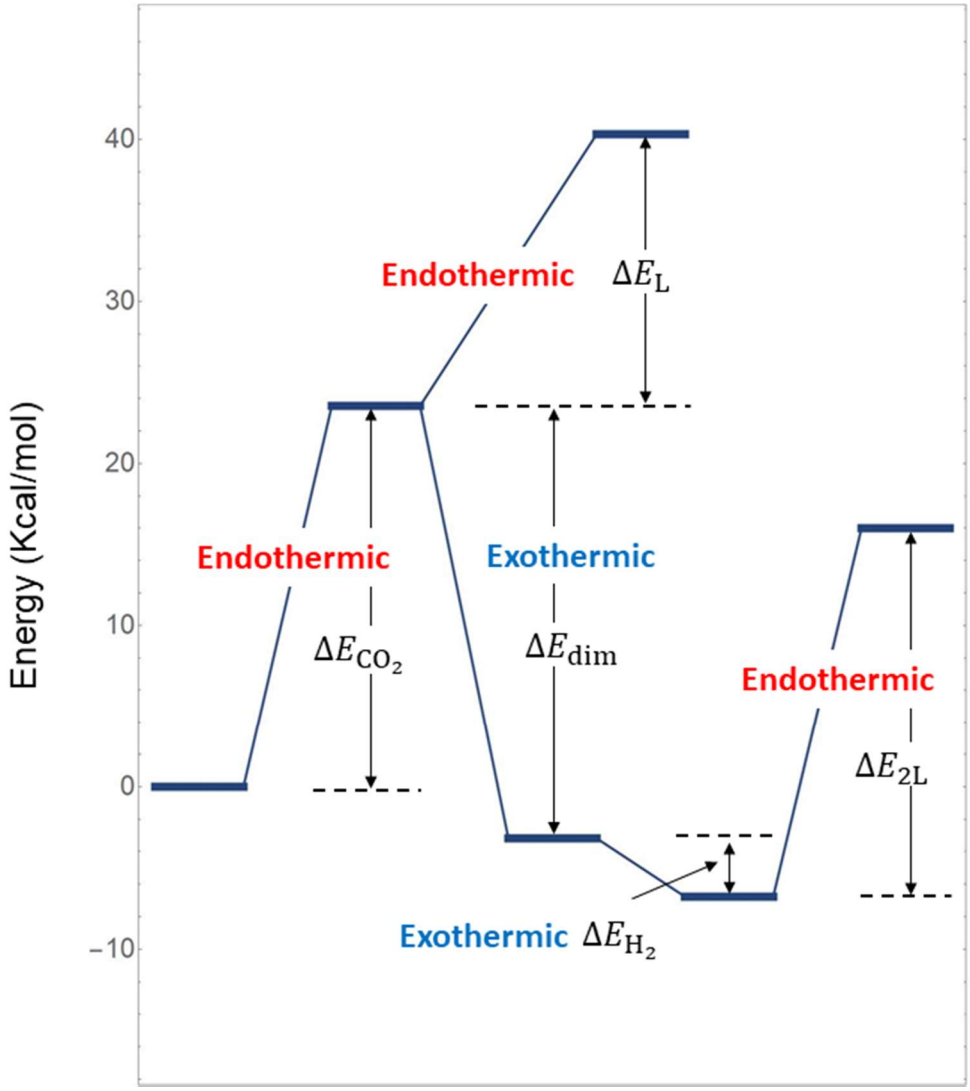

Figure 4. Calculated energy level diagram upon heating of the copper-formate-PA complex.

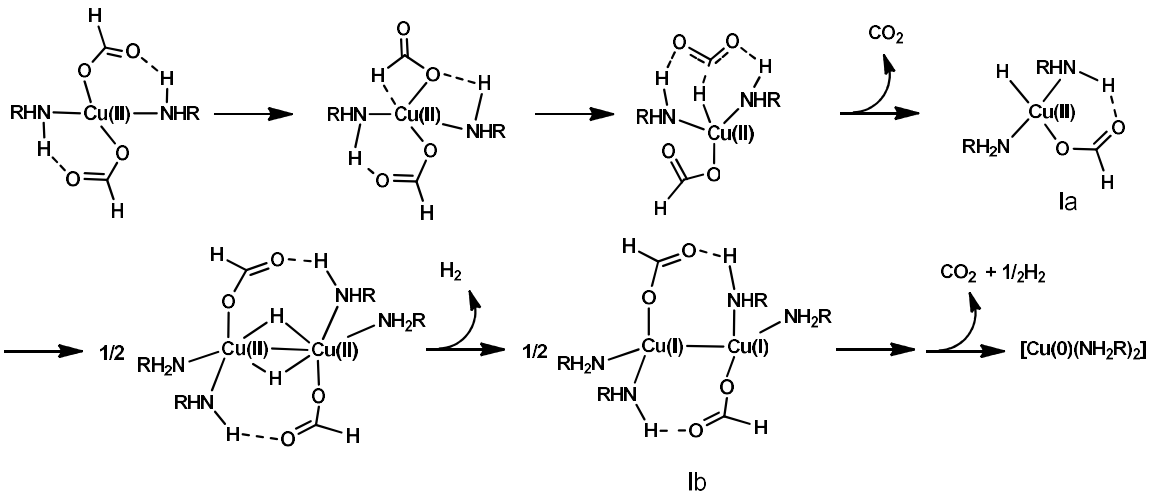

Scheme 1. Proposed mechanism for the dehydrogenation of formate from copper (II) formate coordinated with primary amines

The calculated enthalpy changes at each reaction step for the three different Cu-amine compounds are compared in Table 1. Ligand dissociations from both the monomeric Cu(II)-hydride (ΔE_L) and the dimeric Cu(I) compound (ΔE_{2L}) were found to be endothermic for all three classes of compounds. The binding energy of the ligand (per ligand) to the copper center was greater for the monomeric complex in comparison to the dimeric complex, implying that amine ligands are likely eliminated at the dimeric stage. More specifically, an appreciable decrease of ~43% in the binding energy of the ligand on the dimer in comparison to the monomer was calculated for the case of SA, whereas the decrease of 32% and 28% were found for the PA or PYR cases, respectively. The order of binding strength was determined to be Cu-PA > Cu-SA > Cu-PYR, which means that the ligand dissociation is not entirely attributable to the electronic structure of Cu-N bonds, as predicted from the basicity strength whose order is known as SA > PA > PYR, but rather is influenced by the combination of factors including steric hindrance, hydrogen bonds and coordinating properties. For all three ligand groups, the strong thermodynamic stability of the dimeric Cu(I) compounds was observed as both ΔE_{dim} and ΔE_{H_2} were found to be negative. These Cu(I)-formate dimers are the precursors to Cu particles. As the amines play a part in stabilizing the Cu(I) dimeric species, the ability of the amines to stabilize the Cu(I) species further influences the nucleation of copper particles and affects the particle size as well as size distribution during the metallization from these complexes. The steric interactions caused by amines influence the stability of the dimeric Cu(I) species, which in turn affects the amine coordination strengths. The

relatively lower stability of the dimeric Cu(I)-SA compared to Cu(I)-PA complex is possibly due to the larger steric hindrance of secondary amine at the dimeric stage, which weakens their coordination strength resulting in lower energy costs for ligand dissociation of SA rather than that of PA. These observations are consistent with our previous study that showed that amine ligands with high steric hindrance (Cu-SA) provide less stability to growing copper particles which in turn generate copper particles with higher polydispersity.[8]

Recent work has shown that di-nuclear copper complexes have the potential to be effective catalysts for the dehydrogenation of formic acid, which would effectively enable formic acid as a H_2 carrier for long distance transportation.[40] The current study shows that, post decarboxylation, the monomeric copper hydride is energetically favored to cluster into dimeric copper complexes stabilized by ligands. We note that copper is unusual in this regard when compared to previous calculations for the hydrides of Fe,[35-36] Ni,[39] and Ir.[33] For these species, the monomeric metal hydrides are observed as the thermodynamically favored species upon decarboxylation. Our results imply that the catalytic cycles of copper formate compounds involve the formation of dimeric Cu(II) species as a result of the relative instability of the monomeric Cu(II)-hydride species.

Kcal/mol	ΔE_{CO_2}	ΔE_L	ΔE_{dim}	ΔE_{H_2}	ΔE_{2L}
Cu-PA	23.6	16.8	-26.7	-3.6	22.8
Cu-SA	23.4	15.5	-20.9	-4.2	17.8
Cu-PYR	19.9	7.9	-38.4	-3.0	11.3

Table 1. Comparison of energy levels among Cu-PA, Cu-SA, and Cu-PYR

DSC and TGA-FTIR-MS measurements

The thermal decomposition of bis(octylamine) copper formate (Cu-OCT), was analyzed using differential scanning calorimetry (DSC) along with TGA coupled to FTIR and MS to gain insight into the thermochemistry of the reaction pathway. In Figure 5, DSC curves are plotted together with the released products as detected by TGA-FTIR-MS to illustrate that an endotherm

is observed at the onset of thermolysis, followed by an exotherm and a second endotherm at higher temperatures (the very first two endotherms are melting endotherms. See also Figure S10 that demonstrates the corresponding phase transitions). The first endotherm associated with the thermolysis of Cu-OCT occurs in the same temperature range as the first gaseous product released, CO_2.[8] The concurrence of the endotherm and the release of CO_2, is in agreement with our calculations identifying this step as the rate-determining rotation of the formate to an H-bound configuration. Subsequent to the endothermic release of CO_2, an exothermic peak is observed in concert with the releases of H_2, consistent with our predicted mechanism of copper hydride dimerization (with the possibility of further growth to trimerization and polymerization) and H_2 generation. The exothermic peak has previously been assigned to the dissociation of carbonyl from the Cu(II) complexes, leading to the reduction of Cu(II). [9,41] Our calculation clearly shows that the direct dissociation of a neutral radical HCOO as a single reaction step is not energetically favorable, in comparison to our proposed sequence of reactions where formate is oxidized to form CO2 and H2 and Cu(II) reduced to Cu(I). The endotherm that follows at higher temperature coincides with the release of the ligands, a feature supported by our calculations and other experimental analysis.[9,41] We note that our calculations identified the thermodynamic origin of exothermic and endothermic reactions and their sequence during decomposition, which has not been clearly characterized in previous experimental studies. As shown in Figures S6 and S7, other copper formate compounds revealed similar sequences of endo- and exotherms in concurrence with the release of CO_2, H_2 and their respective ligands; however, the DSC peak intensities varied from compound to compound. Differences in DSC peak intensities among the compounds are rationalized by the differences in the superposition of peaks originating from several processes, including the release of CO_2, H_2, and ligands, from the two step reduction of Cu(II) to Cu(I) and Cu(I) to Cu(0). For example, in the case of copper formate coordinated with 3,5-dimethylpiperidine, its exothermic peak is subdued by two endothermic processes: CO_2 generation at lower temperatures and ligand release at higher temperatures (see Figure S6). Overall, the TGA-FTIR-MS results confirmed that the sequence of reaction products to be released is CO_2 dissociation → H_2 generation (via dimerization) → amine ligands dissociation, which is in agreement with the calculated sequence.

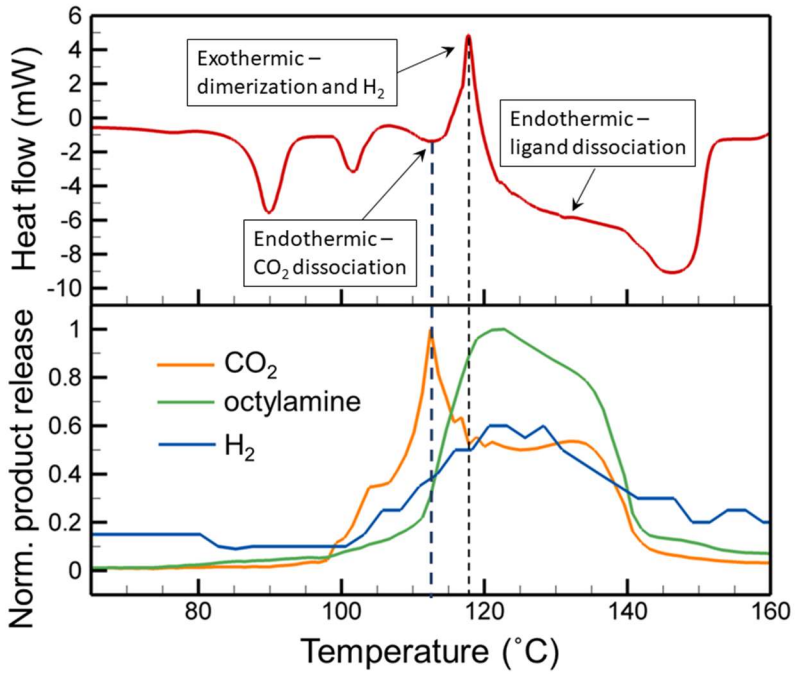

Figure 5. DSC TGA-FTIR-MS curves of the thermolysis of bis(octylamine) copper formate performed at 5°C/min under argon. The first two endothermic peaks are assigned to the melting of the polymorph structure of Cu-OCT compound.

NMR studies of Cu(I)-formate formation and dimerization

Multiple NMR experiments were performed for the Cu-OCT complexes. Due to the paramagnetic nature of the d^9 copper center of these complexes, substantial line broadening is observed and structural changes cannot be easily elucidated for the Cu(II) species. However, with gradual heating to facilitate the first reduction step, a diamagnetic d^{10} Cu(I) species is generated that is amenable to NMR analysis. In our first NMR study, ^{1}H NMR was used to monitor reaction products resulting from heating Cu-OCT in deuterated dimethylsulfoxide (DMSO-d_6) to 80ºC *in situ*, as shown in Figure 6. At room temperature no formate proton signal was observed as all peaks were very broad. After heating at 80ºC for 6 minutes, a peak at 8.02 ppm appeared and gradually increased. This proton resonance is comparable with that of reported proton shifts for Cu(I) formate.[42]** Shortly after, the onset of the second resonance signal at 4.62 ppm appeared and was assigned to the H_2 proton resonance.[43] These results indicate that the generation of H_2 occurs when the Cu(II) species are transformed to Cu(I) and occurs prior to any Cu(0) formation. After heating at 80ºC for 36 minutes, the intensity of the hydrogen signal significantly increased compared to that of the formate proton signal, indicating further conversion of Cu(I) to Cu(0) with

the generation of additional hydrogen molecules. We observed that if the same reaction mixture was heated continuously at 80ºC, the blue solution gradually became colorless (Cu(I)-formate species) followed by precipitation of metallic copper coated on the NMR tube wall, confirming the reaction of Cu(I) to Cu(0) and validating the origin of the increase in the hydrogen signal to the second step in reduction of copper. The small peak at 5.70 ppm in Figure 6 is unknown, though it may represent a N-H resonance signal of carbamate species, which could shift from 1.46 to 6.74 ppm.[44]

^{13}C NMR experiments were subsequently performed and no CO_2 signal was detected in the reaction mixture (see Figure S8 a). Instead, two broad resonances (165.8 ppm and 157.3 ppm) and one sharp carbonyl signal (160.4 ppm) were observed. It is well known that CO_2 readily reacts with amines reversibly to form alkylammonium alkylcarbamates (165.8 ppm) and/or carbamic acids (157.3 ppm).[45-47] Therefore, it is reasonable to assume that the CO_2 released was captured by the amine to form an equilibrium of octylammonium octylcarbamate and octylcarbamic acid, a reaction likely to take place in a sealed NMR tube, but less likely to occur in an open system such as an oven where inks are sintered into copper films. The remaining small, sharp carbonyl signal was assigned to that from the residual Cu(I)-formate. For more direct evidence of CO_2 formation, ^{13}C NMR was used to monitor bis(pyridine) copper formate complexes (Cu-Py) in DMSO-d_6 at 90ºC, as pyridine is less reactive toward CO_2. When the mixture was heated at 90 ºC for 5 minutes, ^{13}C NMR clearly shows the formation of CO_2 with a signal at 124.2ppm (see Figure S8 b).[43] These results indicate that as the Cu(I)-formate species forms (*e.g.* colorless solution), one of the two formates on the copper compound undergoes decarboxylation. Taken together, the ^{1}H NMR and ^{13}C NMR studies revealed that a new colorless Cu(I)-formate species forms during the heating of the sample at 80ºC, accompanied by the generation of CO_2 and H_2. Importantly, both H_2 and CO_2 were observed prior to the reduction of Cu(I)-formate to Cu(0), which agrees with our TGA-FTIR-MS experiment and DFT calculation results.

As previously reported,[48] Cu(I)-formate compounds are not stable in solution but can be stabilized by hydrogen bonding with the excess of formic acid.[43,49] Interestingly, we observed that the stronger the coordinating solvent, the better the Cu(I)-formate species were stabilized with increasing stability in the order of toluene < acetonitrile (CH_3CN) < DMSO, as judged by their relative rates of decompositions from the Cu(I)-formate species to metallic copper. This observation also highlights that the proposed mechanism should only be considered for systems

that do not have secondary species capable of H-bonding that could influence the reaction pathway. For instance, protic solvents or the use of amino alcohols ligands could weaken the amine to formate interaction by forming H-bonding between the ligand and solvent. Conversely, protic solvent could also form hydrogen bonds with the formate or coordinate to the Cu center, which could affect the reaction pathway.

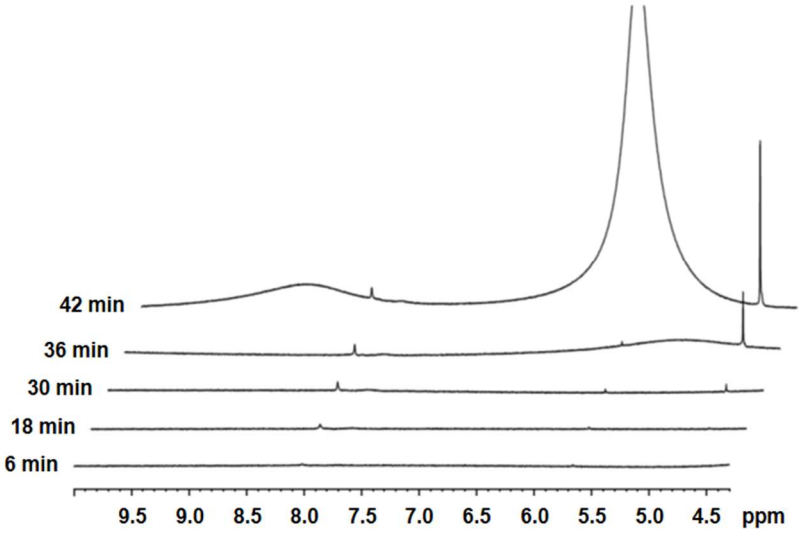

Figure 6 ^{1}HNMR spectra of Cu-OCT as a function of temperature illustrating the concurrent formation of a new formate species (8.02 ppm) along with the generation of H_2 (4.62 ppm).

An additional NMR experiment was performed to determine whether H_2 is generated by dimerizing two separate Cu(II)-hydride species via an intermolecular interaction, or whether a monomeric Cu(II) hydride undergoes a secondary decarboxylation reaction to form a Cu(II)-dihydride species which then liberates H_2 via an intramolecular process. The NMR study used unlabeled and deuterium labeled formates, $Cu(O_2CH)_2(C_8H_{17}NH_2)_2$, and $Cu(O_2CD)_2(C_8H_{17}NH_2)_2$, respectively (referred to as Cu-OCT and Cu-OCT_D). The Cu-OCT was heated to 90°C until a sharp singlet at 4.62 ppm was observed, corresponding to molecular hydrogen formation during the reduction of Cu(II) to Cu(I). Using the same conditions, a mixture composed of a 1:1 molar ratio of Cu-OCT and Cu-OCT_D was heated at 90°C for 35 minutes, which produced the same H_2 singlet at 4.62 ppm as well as a 1:1:1 triplet at 4.57 ppm, as shown in Figure S9. The heteronuclear coupling (J_{HD} = 42.6 Hz) in addition to the slight isotopic shift are indicative of the formation of

HD gas.[50]* The presence of HD clearly indicates that the dehydrogenation step proceeds via an intermolecular interaction and supports the theoretical prediction of dimerization being the preferred pathway (see Scheme S1). Furthermore, when the experiment is performed with Cu-OCT_D, no resonance is observed at 4.62 ppm. This observation provides further evidence that the Cu(II) reduction occurs by the dehydrogenation of formate and not by the oxidation of amines, which has been commonly reported in similar noble metal systems.[44,51]

Collectively, these results provide a set of design principles for the synthesis of high performing copper molecular inks employing copper-formate compounds. The temperature required to sinter copper-formate inks into a metal film is dictated by activation energy of formate oxidation, a step in which the barrier increases with the availability of hydrogen bonding between the amine and the formate. Therefore, copper formate compounds using amines with no possibility of hydrogen bonding are required for milder processing conditions to convert into metallic copper compared to amines that can form hydrogen bonds. Mild sintering conditions provide two advantages: they render the inks compatible with low cost substrates, such as PET and polycarbonate, and they minimize the formation of copper oxides leading to copper films with higher electrical conductance. However, we also show that in the subsequent steps, the same ligands stabilize dimers that form upon copper reduction. These dimers are likely the precursors to longer oligomers and nucleated copper particles. As shown in the experimental and calculated results, ligands that increase the activation barriers of the rate determining step are those that stabilize dimers, resulting in a trade-off between achieving low sintering temperatures and controlled particle nucleation that yields small particles and more uniform particle packing associated with high conductivity films. A review of previous reports comparing various alkylamines shows that how these effects play out in determining the electrical conductivity of copper films. Yabuki et al. found octylamine ligands generated uniform films with low resistivity (~10×10^{-5} Ω·cm) while dibutylamine yielded films made with large particles and resistivity values an order of magnitude higher.[2] We have shown that despite possessing lower decomposition temperatures, copper formates made with secondary and pyridine ligands generated films with higher resistivity (~10^{-4} to 10^{-3} Ω·cm) than those made with primary amines (~10^{-5} Ω·cm), an effect attributed to the weak stabilization by the ligands that leave copper intermediates susceptible to oxidation and to coalescing into large particles or with large cracks and poor film uniformity.[8] Bidendate ligands with low H-bond capacity could provide low sintering temperatures with

increased particle stability. Evidence for the advantageous properties of bidendate ligands have been reported with ethylenediamine ligands yielding uniform particle films with less oxides, an indication that these ligands improve the stability of intermediates.[23,52] These films could be sintered in air to yield films with resistivity values as low as 1.8×10^{-5} Ω·cm and were demonstrated as flexible conductors for LED lights.[23] Opportunities may exist to balance these two opposing effects by using mixtures of ligands [2,7,9] or by adding conductive fillers[53-54] as has been reported previously. Using mixture of ligands has also been successfully used to balance the need for low temperature sintering and stabilization of intermediates.[2,7,9] For instance, mixtures of primary and secondary amines were shown to have improved resistivity values reaching as low as 5×10^{-6} Ω·cm (or ~ 3x bulk values) over using the pure amines alone.[2] A balance between low temperature sintering and good film forming properties was shown possible by mixing primary amines with pyridine ligands.[7] The use of primary amines with copper formate and nanowires were also shown to benefit conductivity over other amines with resistivity values of 12×10^{-6} Ω·cm and use of these inks as to form antennas.[54]

**Based on the integration of the spectra, the ratio of H_2 to HD is more than the simplified statistical prediction (50% HD, 25% H_2, 25% D_2). This deviation can be rationalized by the primary kinetic isotope effect retarding the deuteride formation relative to the hydride formation, yielding a molar ratio closer to 1:1.*

***Comparisons between reaction temperatures found using NMR and DSC could not be made as the heating profiles for each experiment is different.*

CONCLUSION

Amine ligands coordinated to copper-formate compounds direct the mechanistic pathways of thermal decomposition leading to nucleation and growth of copper particles to generate conductive films. Supported by electronic structure calculations and experimental evidence, the current work demonstrates for the first time that the non-covalent interactions, *i.e.*, the hydrogen bonds between amine and the formate ligands, guide the release of CO_2 by determining the activation energy barrier in the rate determining step in the thermal decomposition of bis(amino) copper formate compounds. We also elucidated their mechanistic pathway at the initial nucleation stage of copper particles, *i.e.*, *dimerization* of Cu(II) hydride in concert with the release of H_2, which leads to the exothermic self-reduction of Cu(II) to Cu(I) producing thermodynamically

stable binuclear Cu(I) species. The reactivity towards H_2 generation and reduction of Cu(II) to Cu(I) compounds is facilitated by the thermodynamic stability of the *dimeric* Cu(II) and Cu(I) species, which are greatly affected by the types of amine ligands. These mechanistic studies will provide molecular design guidance with respect to amine ligand groups coordinated to metal-formate complexes in order to achieve optimized molecular inks for printed electronics.

EXPERIMENTAL SECTION

Computational details. The optimized geometries of monomeric and dimeric compounds including reactants and products were calculated by density functional theory (DFT) using the generalized gradient approximation (GGA) with the Perdew-Burke-Ernzehof (PBE) exchange-correlation functional[55] as implemented in the Vienna *Ab initio* Simulation Package (VASP).[56] The basis set consisted of plane waves with a cutoff energy of 600eV, and projector-augmented wave (PAW) method with the frozen core approximation was used.[57] The integration over the Brillouin zone was performed using the Monkhorst-Pack method with a 1 x 1 x 1 *k*-point grid and the dimension of the supercell were 30Å x 30Å x 30Å to avoid the interactions between periodic images. For monomeric Cu(II) complexes, spin-polarized calculations were performed. All structures presented in this paper were fully optimized by relaxing all the atomic coordinates using the conjugated-gradient algorithm until the residual force became less than 0.01 eV/Å. The transition states were obtained by using the climbing-image nudged elastic band (NEB) method.[58-59] A total of 4 intermediate images were used and their minimum energy pathways were calculated by using QM (quick-min) force-based optimizers with the force convergence criteria of 0.03eV/Å. All transition states were ensured by the existence of a single imaginary frequency, using the B3LYP functional[60] with the basis set of TZVP.[61]

Materials. Copper (II) formate dihydrate and tetrahydrate were purchased from Strem Chemicals Inc. or Alpha Aesar. Formic-d_1 acid (95% w/w in H_2O) was purchased from CDN Isotopes. All amines and solvents were purchased from Sigma-Aldrich.

Synthesis of bis(amino) copper formates. Details of the preparation and characterization of the various copper formate compounds can be found elsewhere.[8]

Synthesis of copper (ii) formate-d_2 tetrahydrate. To a stirred suspension of basic copper (ii) carbonate (1 g, 4.52 mmol) in 10 mL of water was slowly added formic-d_1 acid (1.4 mL, 36.34

mmol). Upon addition of the acid the solution takes on a royal blue color accompanied by the rapid evolution of CO_2 gas. After complete addition of the acid the reaction mixture was allowed to stir for 30 min, during which some of the product began to precipitate. The reaction mixture was heated until all the product was dissolved and then stored at 4°C for 24 hrs to afford large cubic crystals of copper (ii) formate-d_2 tetrahydrate that were aquamarine in colour (Yield = 1.2 g, 5.32 mmol, 59%).

Characterization. Coupled analyses of thermogravimetry (TG) and absorption spectroscopy in the mid-infrared region were performed on a Netzsch TG 209 F1 Iris R coupled to a Bruker Tensor 27 Fourier transform infrared (FTIR) spectrometer via a TGA A588 TGA-IR module. The system was run with BOC HP argon (grade 5.3) gas, and residual oxygen was trapped with a Supelco Big-Supelpure oxygen/water trap. Transfer lines between the TG instrument and FTIR spectrometer were heated to a temperature of 200 °C. The release profiles of volatile reaction products were acquired by integrating the FTIR signal in a range of frequencies associated with either the CO_2 vibrational mode, the methylene bending mode or the amine or pyridine ring stretching mode as a function of temperature. More specifically, for the CO_2 release curves, the absorbance between 2200-2450 cm^{-1} was integrated at each temperature and plotted as a function of temperature thereby representing the desorption of CO_2. The ligand-release curves were acquired by integrating the signal at frequencies of 1440-1480 cm^{-1} (for amines) or 1590-1610 cm^{-1} (for pyridine). MS analysis of evolved gases was performed on a Netzsch QMS 403C Aelos coupled to a TG instrument via a transfer line heated to 200 °C. The 2+ mass number was used to track the release of H2. The differential scanning calorimetry (DSC) experiments were done using a TA Instruments DSC model Q2000. The calorimeter was calibrated with Indium and tin at 156.6 °C and 231.9 °C, respectively. The samples were inserted into an aluminum T-zero pan with no lid. The DSC cell was purged with 50 cc/min nitrogen gas and heated at a constant heating ramp of 1 °C per minute from room temperature to 300 °C. NMR spectra were obtained using a Bruker AVANCE 400 MHz NMR Spectrometer. The residual solvent peaks for each NMR experiment were used as the internal standards. All NMR samples were prepared in a nitrogen filled glovebox maintained at less than 0.1 ppm O_2 and less than 2 ppm H_2O and NMR tubes were sealed with Teflon taps prior to analysis.

SUPPORTING INFORMATION

Optimized structures of dimer compounds, TGA-FTIR-MS and DSC data, NMR spectra, proposed catalytic cycle of copper formate compounds.

AUTHOR INFORMATION

Corresponding Author

*Homin.Shin@nrc-cnrc.gc.ca

**Chantal.Paquet@nrc-cnrc.gc.ca

ACKNOWLEDGMENT

The authors wish to thank Malgosia Daroszewska and Gilles Robertson for the contribution on the thermal analysis experiments. MS thanks the Natural Sciences and Engineering Research Council Discovery Grants program for funding support.

REFERENCES

[1] Yabuki, A.; Arriffin, N.; Yanase, M. Low-Temperature Synthesis of Copper Conductive Film by Thermal Decomposition of Copper–Amine complexes. *Thin Solid Films* **2011**, *519*, 6530-6533.

[2] Yabuki, A.; Tanaka, S. Electrically Conductive Copper Film Prepared at Low Temperature by Thermal Decomposition of Copper Amine Complexes with Various Amines. *Mater. Res. Bull.* **2012**, *47*, 4107-4111.

[3] Shin, D. H.; Woo, S.; Yem, H.; Cha, M.; Cho, S.; Kang, M.; Jeong, S.; Kim, Y.; Kang, K.; Piao, Y. A Self-Reducible and Alcohol-Soluble Copper-Based Metal−Organic Decomposition Ink for Printed Electronics. *ACS Appl. Mater. Interfaces* **2014**, *6*, 3312-3319.

[4] Yabuki, A.; Tachibana, Y.; Fathona, I. W. Synthesis of Copper Conductive Film by Low-Temperature Thermal Decomposition of Copper-Aminediol Complexes under an Air Atmosphere. *Mater. Chem. Phys.* **2014**, *148*, 299-304.

[5] Choi, Y. H.; Hong, S. H. Effect of the Amine Concentration on Phase Evolution and Densification in Printed Films Using Cu(II) Complex Ink. *Langmuir* **2015**, *31*, 8101-8110.

[6] Cho, S.; Yin, Z.; Ahn, Y.; Piao, Y.; Yoo, J.; Kim, Y. S. Self-Reducible Copper Ion Complex Ink for Air Sinterable Conductive Electrodes. *J. Mater. Chem. C* **2016**, *4*, 10740-10746.

[7] Paquet, C.; Lacelle, T.; Deore, B.; Kell, A. J.; Liu, X.; Korobkov, I.; Malenfant, P. R. L. Pyridine–Copper(II) Formates for the Generation of High Conductivity Copper Films at Low Temperatures. *Chem. Commun.* **2016**, *52*, 2605-2608.

[8] Paquet, C.; Lacelle, T.; Liu, X.; Deore, B.; Kell, A. J.; Lafrenière, S.; Malenfant, P. R. L. The Role of Amine Ligands in Governing Film Morphology and Electrical Properties of Copper Films Derived from Copper Formate-Based Molecular Inks. *Nanoscale* **2018**, *10*, 6911-6921.

[9] Xu, W.; Wang, T. Synergetic Effect of Blended Alkylamines for Copper Complex Ink To Form Conductive Copper Films. *Langmuir* **2017**, *33*, 82-90.

[10] Farraj, Y.; Smooha, A.; Kamyshny, A.; Magdassi S. Plasma-Induced Decomposition of Copper Complex Ink for the Formation of Highly Conductive Copper Tracks on Heat-Sensitive Substrates. *ACS Appl. Mater. Interfaces* **2017**, *9*, 8766.

[11] Farraj, Y.; Layani, M.; Yaverboim, A.; Magdassi S. Binuclear Copper Complex Ink as a Seed for Electroless Copper Plating Yielding >70% Bulk Conductivity on 3D Printed Polymers. *Adv. Mater. Interfaces* **2018**, *5*, 1701285.

[12] Marchal, W.; Longo, A.; Briois, V.; Van Hecke, K. V.; Elen, K.; Van Bael, M. K.; Hardy, A. Understanding the Importance of Cu(I) Intermediates in Self-Reducing Molecular Inks for Flexible Electronics. *Inorg. Chem.* **2018**, *57*, 15205-15215.

[13] Deore, B.; Paquet, C.; Kell, A. J.; Lacelle, T.; Liu, X.; Mozenson, O.; Lopinski, G.; Brzezina, G.; Guo, C.; Lafreniere, S.; Malenfant, P. R. L. Formulation of Screen-Printable Cu Molecular Ink for Conductive/Flexible/Solderable Cu Traces. *ACS Appl. Mater. Interfaces* **2019**, *11*, 38880-38894.

[14] Oliva-Puigdomenech, A.; Roo, J. D.; Kujs, J.; Detavernier, C.; Martins, J. C.; Hens, Z. Ligand Binding to Copper Nanocrystals: Amines and Carboxylic Acids and the Role of Surface Oxides. *Chem. Mater.* **2019**, *31*, 2058-2067.

[15] Li, W.; Sun, Q.; Li, L.; Jiu, J.; Liu, X.-Y.; Kanehara, M.; Minari, T.; Suganuma, K. The Rise of Conductive Copper Inks: Challenges and Perspectives. *Appl. Mater. Today* **2020**, *18*, 100451.

[16] Adner, D.; Wolf, F. M.; Möckel, S.; Perelaer, J.; Schubert, U. S.; Lang, H. Copper(II) Ethylene Glycol Carboxylates as Precursors for Inkjet Printing of Conductive Copper Patterns. *Thin Solid Films* **2014**, *565*, 143-148.

[17] Deng, D.; Qi, T.; Cheng, Y.; Jin, Y.; Xiao, F. Copper Carboxylate with Different Carbon Chain Lengths as Metal–Organic Decomposition Ink. *J. Mater. Sci. Mater. Electron.* **2014**, *25*, 390-397.

[18] Yong, Y.; Nguyen, M. T.; Tsukamoto, H.; Matsubara, M.; Liao, Y.C.; Yonezawa, T. Effect of Decomposition and Organic Residues on Resistivity of Copper Films Fabricated via Low Temperature Sintering of Complex Particle Mixed Dispersions. *Sci. Rep.* **2017**, *7*, 45150.

[19] Kim, S. J.; Lee, J.; Choi, Y. -H.; Yeon, D. -H.; Byun, Y. Effect of Copper Concentration in Printable Copper Inks on Film Fabrication. *Thin Solid Films* **2012**, *520*, 2731-2734.

[20] Lee, Y.-I.; Lee, K.-J.; Goo, Y.-S.; Kim, N.-W.; Byun, Y.; Kim, J.-D.; Yoo, B.; Choa, Y.-H. Effect of Complex Agent on Characteristics of Copper Conductive Pattern Formed by Ink-jet Printing. *Jpn. J. Appl. Phys.* **2010**, *49*, 86501.

[21] Yang, W.; Liu, C.; Zhang, Z.; Liu, Y.; Nie, S. Copper Inks Formed Using Short Carbon Chain Organic Cu-Precursors. *RSC Adv.* **2014**, *4*, 60144-60147.

[22] Chotipanich, J.; Hanim, S.; Bakar, A.; Arponwichanop, A.; Yonezawa, T.; Kheawhom, S. Copper Conductive Patterns Through Spray-Pyrolysis of Copper-Diethanolamine Complex Solution. *PLoS ONE* **2018**, *13*, e0200084.

[23] Dong, Y.; Lin, Z.; Li, X.; Zhu, Q.; Li, J.- G.; Sun, Z. A Low Temperature and Air-sinterable Copper-diamine Complex-based Metal Organic Decomposition Ink for Printed Electronics. *J. Mater. Chem. C* **2018**, *6*, 6406-6415.

[24] Rosen, Y.; Marrach, R.; Gutkin, V.; Magdassi, S. Thin Copper Flakes for Conductive Inks Prepared by Decomposition of Copper Formate and Ultrafine Wet Milling. *Adv. Mater. Technol.* **2019**, *4*, 1800426.

[25] Galwey, A. K.; Jamleson, D. M.; Brown, M. E. Thermal Decomposition of Three Crystalline Modifications of Anhydrous Copper(II) Formate. *J. Phys. Chem.* **1974**, *78*, 2664-2670.

[26] Mohamed, M. A.; Galwey, A. K.; Halawy, S. A. Kinetic and Thermodynamic Studies of the Nonisothermal Decomposition of Anhydrous Copper(II) Formate in Different Gas Atmospheres. *Thermochimica Acta* **2004**, *411*, 13-20.

[27] Sordakis, K.; Tang, C.; Vogt, L. K.; Junge, H.; Dyson, P. J.; Beller, M.; Laurenczy, G. Homogeneous Catalysis for Sustainable Hydrogen Storage in Formic Acid and Alcohols. *Chem. Rev.* **2018**, *118*, 372-433.

[28] Scotti, N.; Psaro, R.; Ravasio, N.; Zaccheria, F. A New Cu-Based System for Formic Acid Dehydrogenation. *RSC Adv.* **2014**, *4*, 61514-61517.

[29] Correa, A.; Cascella, M.; Scotti, N.; Zaccheria, F.; Ravasio, N.; Psaro, R. Mechanistic Insights into Formic Acid Dehydrogenation Promoted by Cu-Amino Based Systems. *Inorganica Chim. Acta* **2018**, *470*, 290-294.

[30] Barclay, G. A.; Kennard, C. H. L. The Crystal Structure of Anhydrous Copper(II) Formate. *J. Chem. Soc.* **1961**, *78*, 3289-3294.

[31] In this study, we mainly calculated for these three representative amines as our minimal model due to computational cost. The chain length effect appeared not to be significant, as shown in the calculation result with full molecular amines (octylamine vs. 3-butylpyridine) (see Figure S2 and S3).

[32] Koh, K.; Jeon, M.; Yoon, C. W.; Asefa, T. Formic Acid Dehydrogenation over Pd NPs Supported on Amine-Functionalized SBA-15 Catalysts: Structure–Activity Relationships. *J. Mater. Chem. A* **2017**, *5*, 16150-16161.

[33] Oldenhof, S.; Lutz, M.; de Bruin, B.; van der Vlugt, J. I.; Reek, J. N. H. Dehydrogenation of Formic Acid by Ir–bisMETAMORPhos Complexes: Experimental and Computational Insight Into the Role of a Cooperative Ligand. *Chem. Sci.* **2015**, *6*, 1027-1034.

[34] Schmeier, T. J.; Dobereiner, G. E.; Crabtree, R. H.; Hazari, N. Secondary Coordination Sphere Interactions Facilitate the Insertion Step in an Iridium(III) CO_2 Reduction Catalyst. J. Am. Chem. Soc. **2011**, *133*, 9274-9277.

[35] Zell, T.; Butschke, B.; Ben-David, Y.; Milstein, D. Efficient Hydrogen Liberation from Formic Acid Catalyzed by a Well-Defined Iron Pincer Complex under Mild Conditions. *Chem. Eur. J.* **2013**, *19*, 8068-8072.

[36] Yang, X. Mechanistic Insights into Iron Catalyzed Dehydrogenation of Formic Acid: β-Hydride Elimination vs. Direct Hydride transfer. *Dalton Trans.* **2013**, *42*, 11987-11991.

[37] Bielinski, E. A.; Lagaditis, P. O.; Zhang, Y.; Mercado, B. Q.; Wurtele, C.; Bernskoetter, W. H.; Hazari, N.; Schneider, S. Lewis Acid-Assisted Formic Acid Dehydrogenation Using a Pincer-Supported Iron Catalyst. *J. Am. Chem. Soc.* **2014**, *136*, 10234-10237.

[38] Boddien, A.; Mellmann, D.; Gärtner, F.; Jackstell, R.; Junge, H.; Dyson, P. J.; Laurenczy, G.; Ludwig, R.; Beller, M. Efficient Dehydrogenation of Formic Acid Using an Iron Catalyst. *Science* **2011**, *333*, 1733-1736.

[39] Xue, L.; Ahlquist, M. S. G. A DFT Study: Why Do $[Ni(P^{R}_{2}N^{R'}_{2})_{2}]^{2+}$ Complexes Facilitate the Electrocatalytic Oxidation of Formate? *Inorg. Chem.* **2014**, *53*, 3281-3289.

[40] Nakajima, T.; Kamiryo, Y.; Kishimoto, M.; Imai, K.; Nakamae, K.; Ura, Y.; Tanase, T. Synergistic Cu_2 Catalysts for Formic Acid Dehydrogenation. *J. Am. Chem. Soc.* **2019**, *141*, 8732-8736.

[41] Li, W.; Li, C.-F.; Lang, F.; Jiu, J.; Ueshima, M.; Wang, H.; Liu, Z.-Q.; Suganuma K. Self-Catalyzed Copper–Silver Complex Inks for Low-Cost Fabrication of Highly Oxidation-Resistant and Conductive Copper–Silver Hybrid Tracks at a Low Temperature Below 100 °C. *Nanoscale* **2018**, *10*, 5254-5263.

[42] Tuchscherer, A.; Shen, Y.; Jakob, A.; Mothes, R.; Al-Anber, M.; Walfort, B.; Rüffer, T.; Frühauf, S.; Ecke, R.; Schulz, S. E.; Gessner, T.; Lang, H. Lewis-Base Copper(I) Formates: Synthesis, Reaction Chemistry, Structural Characterization and Their Use as Spin-Coating Precursors for Copper Deposition. *Inorganica Chim. Acta* **2011**, *365*, 10-19.

[43] Fulmer, G. R.; Miller, A. J. M.; Sherden, N. H.; Gottlieb, H. E.; Nudelman, A.; Stoltz, B. M.; Bercaw, J. E.; Goldberg, K. I. NMR Chemical Shifts of Trace Impurities: Common Laboratory Solvents, Organics, and Gases in Deuterated Solvents Relevant to the Organometallic Chemist. *Organometallics* **2010**, *29*, 2176-2179.

[44] Chen, M.; Feng, T. -G.; Wang, X.; Li, T.-C.; Zhang, J.-Y.; Qian, D.-J. Silver Nanoparticles Capped by Oleylamine: Formation, Growth, and Self-Organization. *Langmuir* **2007**, *10*, 5296-5304.

[45] George, M.; Weiss, R. G. Detection of Pre-Sol Aggregation and Carbon Dioxide Scrambling in Alkylammonium Alkylcarbamate Gelators by Nuclear Magnetic Resonance. *Langmuir* **2003**, *19*, 8168-8176.

[46] Barzagli, F.; Mani, F.; Peruzzini, M. Carbon Dioxide Uptake as Ammonia and Amine Carbamates and Their Efficient Conversion into Urea and 1,3-Disubstituted ureas. *J CO2 UTIL* **2016**, *13*, 81-89.

[47] Hampe, E. M.; Rudkevich, D. M. Exploring Reversible Reactions between CO_2 and Amines. *Tetrahedron* **2003**, *59*, 9619-9625.

[48] La Monica, G. ; Ardizzoia, G. A.; Cariati, F.; Cenini, S.; Pizzotti, M. Isolation of Ionic Products in the Reaction of CO_2 with (Tetrahydroborato)copper(I) Complexes: Synthesis and Reactions of $[(biL)(Ph_3P)_2Cu][HB(O_2CH)_3]$ and $[(biL)(Ph_3P)_2Cu][H_2B(O_2CH)_2]$ (biL = 1,10-Phenanthroline, 3,4,7,8-T etramethyl-1,10-phenanthroline). *Inorg. Chem.* **1985**, *24*, 3920-3923.

[49] Lang, H.; Shen, Y.; Rüffer, T.; Walfort, B. Phosphane Copper(I) Formate Complexes Stabilized by Formic Acid and Acetic Acid Through H--O--H bridges. *Inorganica Chim. Acta* **2008**, *361*, 95-102.

[50] Neronov, Y. I.; Karshenboim, S. G. NMR Spectroscopy of Hydrogen Deuteride and Magnetic Moments of Deuteron and Triton. *Phys. Lett. Sect. A* **2003**, *318*, 126-132.

[51] Xu, B.; Hartigan, E. M.; Feula G.; Huang, Z.; Lumb, J.-P.; Arndtsen, B. A. Simple Copper Catalysts for the Aerobic Oxidation of Amines: Selectivity Control by the Counterion. *Angew. Chemie Int. Ed.* **2016**, *55*, 15802-15806.

[52] Marchal, W.; Mattelaer, F.; Van Hecke, K.; Briois, V.; Longo, A.; Reenaers, D.; Elen, K.; Detavernier, C.; Deferme, W.; Van Bael, M. K.; Hardy A. Effectiveness of Ligand Denticity-Dependent Oxidation Protection in Copper MOD Inks Langmuir 2019, 35, 16101−16110.

[53] Li, W.; Cong, S.; Jiu, J.; Nagao S.; Suganuma, K. Self-reducible copper inks composed of copper–amino complexes and preset submicron copper seeds for thick conductive patterns on a flexible substrate J. Mater. Chem. C 2016, 4, 8802-8809.

[54] Zhang, B.; Chen, C.; Li, W.; Yeom, J.; Suganuma, K. Well-Controlled Decomposition of Copper Complex Inks Enabled by Metal Nanowire Networks for Highly Compact, Conductive, and Flexible Copper Films Adv. Mater. Interfaces 2020, 7, 1901550.

[55] Perdew, J. P.; Burke, K.; Ernzerhof, M. Generalized Gradient Approximation Made Simple. *Phys. Rev. Lett.* **1996**, *77*, 3865-3868.

[56] Kresse, G.; Furthmüller, J. Efficient Iterative Schemes for *ab initio* Total-Energy Calculations Using a Plane-Wave Basis Set. *Phys. Rev. B* **1996**, *54*, 11169-11186.

[57] Blöchl, P. E. Projector Augmented-Wave Method. *Phys. Rev. B* **1994**, *50*, 17953-17979.

[58] Henkelman G.; Jónsson, H. A Climbing Image Nudged Elastic Band Method for Finding Saddle Points and Minimum Energy Paths. *J. Chem. Phys.* **2000**, *113*, 9901-9904.

[59] Becke, A. D. Density-Functional Thermochemistry. III. The Role of Exact Exchange. *J. Chem. Phys.* **1993**, *98*, 5648-5652.

[60] Stephens, P. J.; Devlin, F. J.; Chabolowski, C. F.; Frisch, M. J. Ab Initio Calculation of Vibrational Absorption and Circular Dichroism Spectra Using Density Functional Force Fields. *J. Phys. Chem.* **1994**, *98*, 11623-11627.

[61] Schaefer, A.; Huber, C.; Ahlrichs, R. Fully Optimized Contracted Gaussian Basis Sets of Triple Zeta Valence Quality for Atoms Li to Kr. *J. Chem. Phys.*, **1994,** *100*, 5829.

TABLE OF CONTENTS